International Journal of Pharmaceutics 596 (2021) 120263

Contents lists available at ScienceDirect

International Journal of Pharmaceutics

journal homepage: www.elsevier.com/locate/ijpharm

Effects of temperature and relative humidity in D_2O on solid-state hydrogen deuterium exchange mass spectrometry (ssHDX-MS)

Rishabh Tukra [a], Sam Gardner [b], Elizabeth M. Topp [a,c,*]

[a] Department of Industrial and Physical Pharmacy, College of Pharmacy, Purdue University, West Lafayette, IN 47907, United States
[b] Wildstat Consulting LLC, Lafayette, IN 47905, United States
[c] National Institute for Bioprocessing Research and Training, Belfield, Blackrock, Co., Dublin A94 X099, Ireland

ARTICLE INFO

Keywords:
ssHDX-MS
Design of experiments
RH effects
Temperature effects
SAS JMP ® Pro
Myoglobin

ABSTRACT

Lyophilized powders containing myoglobin and various excipients were subjected to ssHDX-MS at different temperatures and D_2O vapor activity (RH). Deuterium incorporation was fitted to a bi-exponential association model for each formulation and the dependence of regression parameters on temperature and RH was evaluated. Data fitted best to a simplified model in which the slow exponential term was considered invariant with temperature and RH while the fast exponential term retained its temperature and RH dependence. This suggests that rapid rate processes such as water vapor sorption and initial deuterium labeling may be more dependent on temperature and RH than slower processes such as sequential exchange and transport in the solid matrix.

1. Introduction

Protein drugs are often marketed as lyophilized solids due to the improved storage stability typically imparted by the solid state. To verify product stability and efficacy, lyophilized protein formulations undergo stability assessments over months or even years. Accelerated stability testing uses elevated temperature and RH conditions to provide a more rapid indication of product performance, but the practical range of temperature and RH conditions that can be used may be limited by the physical properties of the formulation such as the glass transition temperature, and results may not reflect degradation at the intended storage conditions (Lonardo et al., 2012; Rauk et al., 2014). While physical and chemical properties of the formulation such as the glass transition temperature, moisture content and protein secondary structure are routinely measured for these biomolecule formulations, they are often poorly correlated with stability on storage. As a result, 'real time' stability studies remain the gold standard for assessing product quality. To reduce reliance on time-consuming and costly stability testing, advanced analytical methods are needed that adequately characterize the solid matrix and serve as a rapid indicator of protein stability and product quality.

Our group has developed solid state hydrogen deuterium exchange-mass spectrometry (ssHDX-MS) as an analytical method to measure protein structure and matrix interactions in the solid state (Iyer et al., 2016; Moorthy et al., 2015a, 2015b, 2015c, 2014; Moussa et al., 2018). In this technique, uncapped vials containing lyophilized protein formulations are exposed to D_2O vapor at controlled temperature and relative humidity (RH). An increase in the mass of the protein due to the exchange of protons for deuterons at backbone amide groups can be measured using mass spectrometry for both the intact protein and peptic digests (Li et al., 2008; Moorthy et al., 2015c; Sophocleous et al., 2012). The rate and extent of deuterium incorporation in lyophilized proteins has been shown to depend on relative humidity in D_2O, excipient type and processing methods (Li et al., 2008; Sophocleous et al., 2012). Recent studies have also shown that the extent of deuterium incorporation measured by ssHDX-MS in freshly prepared samples is correlated with the aggregation of the protein on extended storage for myoglobin, a monoclonal antibody and an antibody fragment (Moorthy et al., 2018). These results suggest that ssHDX-MS may be useful in ranking protein formulations or processing methods during development, reducing the need for stability studies. Similar approaches have been applied to proteins in frozen solids or adsorbed to solid surfaces, to lyophilized proteins using FTIR rather than MS detection, and to lyophilized proteins in a semi-automated format using MALDI-MS (Fang et al., 2016; Kabaria et al., 2019; Moorthy et al., 2016). The mechanisms of exchange in the solid state are not yet clear, however, and the molecular basis for

* Corresponding author at: Department of Industrial and Physical Pharmacy, College of Pharmacy, Purdue University, 575 Stadium Mall Drive, 47907 West Lafayette, IN, United States.
E-mail address: topp@purdue.edu (E.M. Topp).

https://doi.org/10.1016/j.ijpharm.2021.120263
Received 26 August 2020; Received in revised form 7 January 2021; Accepted 10 January 2021
Available online 21 January 2021

interpreting the rate and extent of deuterium incorporation in ssHDX-MS has not been established.

The results of solution HDX experiments are usually interpreted using the model first proposed by Linderstrøm-Lang and Hvidt, which relates deuterium incorporation to the "opening" and "closing" of the protein structure (i.e., global or partial unfolding and refolding) (Hvidt and Linderstrøm-Lang, 1955, 1954). The Linderstrøm-Lang model assumes that, when a protein is solvated in D_2O, exchange occurs when the protein is in its open state. The deuterated protein then refolds or "closes", and it is assumed that exchange does not occur in the folded form. Mathematically, the Linderstrøm-Lang model relates the rate of deuterium incorporation to the rates of opening (k_{op}) and closing (k_{cl}), and to the intrinsic rate of chemical exchange (k_{ch}) (Eq. (1)). Chemical exchange is assumed to be irreversible.

$$X - H_{closed} \underset{k_{cl}}{\overset{k_{op}}{\rightleftarrows}} X - H_{open} \xrightarrow{k_{ch}} X - D_{open} \underset{k_{op}}{\overset{k_{cl}}{\rightleftarrows}} X - D_{closed} \quad (1)$$

A number of observations suggest that the Linderstrøm-Lang model is not applicable to hydrogen-deuterium exchange in solid samples (ssHDX-MS). For example, recent results from our lab have shown that protection from exchange is observed in ssHDX for unstructured peptides, which cannot unfold and refold (Kammari and Topp, 2019). The Linderstrøm-Lang model predicts that such peptides will not be protected from exchange in solution at all. Similarly, the rate and extent of ssHDX are affected by the relative humidity of D_2O in the vapor phase, a measure of $D_2O_{(g)}$ activity (Li et al., 2007; Sophocleous and Topp, 2012). D_2O activity is not included in the Linderstrøm-Lang model. The time course of an ssHDX experiment is on the order of days to weeks, as opposed to minutes or less for solution HDX. This suggests that the Linderstrøm-Lang assumption that chemical exchange is irreversible may not be valid for ssHDX. Thus, there is a need for a kinetic model for ssHDX-MS that describes experimental observations such as these and supports a mechanistic interpretation of the data.

To address the need for an ssHDX model, the studies reported here examined the effects of excipient type, temperature and D_2O relative humidity (hereinafter, 'RH') on the rate and extent of ssHDX using a statistical approach. Myoglobin was co-lyophilized with different excipients (dextran, sucrose, mannitol, sodium chloride) and exposed to different conditions of temperature and RH. The excipients were selected to represent a range expected properties and protein-excipient interactions: (i) sucrose is a common stabilizing and hydrogen-bond forming excipient in protein formulations, (ii) dextran is a polymeric stabilizer and collapse temperature modifier (Allison et al., 2000; Larsen et al., 2019; Yoshioka et al., 2006) with functional groups similar to those of sucrose and higher molecular weight, (iii) mannitol is a hydrogen-bond forming excipient that often undergoes recrystallization and phase separation (Horn and Friess, 2018; Kulkarni et al., 2018; Lu and Pikal, 2004) which may limit protein-excipient interactions, and (iv) sodium chloride serves as a negative control, and has little to no ability to form hydrogen bonds and may also recrystallize. Deuterium incorporation over time was then measured at the intact protein level using mass spectrometry. Deuterium incorporation kinetics were fitted to a bi-exponential rate law, and the dependences of regression parameters on temperature and RH were explored using the statistical package JMP® Pro.

2. Materials and methods

2.1. Materials

Deuterium oxide (99.9%) was purchased from Cambridge Isotope Laboratories (Andover, MA). Myoglobin from equine skeletal muscle (CAS 100684-32-0, 95-100%) was purchased from Sigma Life Science (St. Louis, MO). The excipient sodium chloride (CAS 7647-14-5) was obtained from Fischer Scientific (Hampton, NH), D-mannitol (CAS 69-65-8) was obtained from Sigma-Aldrich (St. Louis, MO), and dextran (CAS 9004-54-0) and sucrose (CAS 57-50-1) were obtained from Alfa Aesar (Haverhill, MA) and Sigma Life Science, respectively. Salts for controlling RH in the desiccators were purchased from Sigma-Aldrich (lithium bromide and potassium acetate), Fisher Scientific (lithium chloride,) and VWR International (Radnor, PA) (potassium carbonate). Potassium phosphate salts (dibasic and monobasic) were purchased from Sigma-Aldrich. Lyophilization vials (Wheaton serum tubing vials, part 223683) and stoppers (Duran Wheaton Kimble, part W224100-093) were purchased from Fisher Scientific. All mass spectrometric (MS) grade solvents were also obtained from Fisher Scientific.

2.2. Methods

2.2.1. Sample preparation

A stock solution was prepared by dissolving myoglobin in 2.5 mM potassium phosphate buffer (pH 7.4) to produce a 10 mg/mL final protein concentration. This solution was then dialyzed in 2.5 mM pH 7.4 potassium phosphate buffer for 24 h using a Slide-A-Lyzer G2 dialysis cassette (CAS 87731, MWCO 10,000 Da; ThermoFisher, Waltham, MA). During dialysis, the phosphate buffer was replaced with fresh buffer at least once. Excipient (sucrose, dextran, mannitol or sodium chloride) solutions of approximately 50 mg/mL were prepared in the same phosphate buffer. The dialyzed myoglobin solution and the excipient solution were mixed to produce a final concentration of 5 mg/mL each of myoglobin and the excipient. A 0.2 mL aliquot of this final solution was then pipetted into a 2 mL vial and lyophilized using a Lyostar 3 lyophilizer (SP Scientific, Warmister, PA). The lyophilization cycle consisted of freezing at −40 °C, holding for 3 h to ensure freezing; primary drying at −35 °C and holding for 28 h at a vacuum set point of 70 mTorr; and secondary drying at 25 °C for 8 h at a 70 mTorr vacuum set point. At the end of the cycle, the vials were backfilled with nitrogen and then capped and held in the lyophilizer at 5 °C until they were removed.

2.2.2. Experimental design

To explore the effects of temperature and RH on the stability and kinetics of ssHDX-MS, lyophilized myoglobin formulations stored at varying temperature and RH conditions were measured over time with ssHDX-MS using two designed experiments. The first experiment involved the use of sucrose and dextran at four different levels of RH and temperature with a total of seven time points per condition, resulting in a $2 \times 4 \times 4 \times 7$ full factorial design. The second experiment involved the use of mannitol and sodium chloride at three different levels of RH and temperature with a total of seven time points per condition, a $2 \times 3 \times 3 \times 7$ factorial design. The experimental factors are shown in Table 1. The more efficient design of the second experiment was chosen based on the results obtained from the first experiment, which showed that sufficient information on the effects of RH and temperature on ssHDX-MS kinetics could be captured with fewer experimental runs. The statistical approach to data collection and analysis is described in greater detail in Appendix A.

2.2.3. Solid state HDX-MS (ssHDX-MS)

After lyophilization, samples were uncapped and placed inside glass desiccators at controlled RH in D_2O. The RH was controlled using saturated salt solutions (LiBr for 6%RH, LiCl for 11%RH, KCH_3CO_2 for

Table 1
Design of experiments and experimental factors with their levels used in ssHDX-MS experiments.

Factor	Experiment 1 levels	Experiment 2 levels
Excipient	Sucrose, dextran	Mannitol, sodium chloride
Temperature (°C)	5, 15, 25, 40	15, 25, 40
Relative humidity (%)	6, 11, 23, 43	11, 23, 43
Time (h)	3, 6, 12, 24, 48, 120, 240	3, 6, 12, 24, 48, 120, 240

23%RH and K_2CO_3 for 43%RH) in D_2O at the bottom of the desiccator. The salt solution was separated from the vials by a mesh separator and the lid of the desiccator was sealed. In the closed desiccator, D_2O in the solid powder is assumed to be in equilibrium with that in the vapor phase, so that different solid formulations deuterated at the same RH and temperature have identical D_2O activity in the solid phase. To evaluate the effects of both RH and temperature on ssHDX-MS, samples at each of the four RH values were incubated at different temperatures controlled using ovens (Table 1). Three vials were removed from the desiccators at seven different time points and immediately quenched in liquid nitrogen. This corresponds to HDX measurement replication at the level of labeling (i.e., level three of the five levels defined by Moroco and Engen), in that three vials from the same stock solution and lyophilization run were deuterated independently (Moroco and Engen, 2015). The quenched samples were then stored at −80 °C until analysis.

The deuterated samples were analyzed using an Agilent Technologies G6510A Q-TOF LC-MS instrument (Agilent Technologies, Santa Clara, CA). A custom column-switching and refrigeration unit was used to allow for temperature control at 4 °C and to desalt the injected sample. Prior to injection, the samples were reconstituted with 0.2 mL of quench buffer (0.2% v/v formic acid and 5% v/v methanol in MS grade water, pH 2.5) maintained at 4 °C in an ice bath. The LC system had an isocratic flow rate of 0.2 mL/min and a total run time of 10.2 min with a gradient flow consisting of 0.1% formic acid in MS grade water and 0.1% formic acid in MS grade acetonitrile. Mass spectra were acquired over a 500–3200 *m/z* range. An undeuterated control containing myoglobin alone and a fully deuterated control were also analyzed. The fully deuterated control was prepared by diluting a myoglobin solution 1:9 v/v with deuterium oxide and storing at room temperature for 48 h under mild agitation.

All samples were analyzed using MassHunter Workstation software equipped with the BioConfirm package (Agilent Technologies, Version B.04.00). The masses of deuterated myoglobin thus obtained were plotted using GraphPad Prism 8 graphing software (GraphPad Software, San Diego, CA. version 8.1.0). The masses obtained from the LC-MS analyses were corrected for back exchange against the fully deuterated myoglobin sample using the formula:

$$D(\%) = \frac{(M_t - M_0)}{(M_{100} - M_0)} \times 100 \quad (2)$$

where *D(%)* is the percentage deuterium uptake at time *t*, M_t is the mass of myoglobin at various time points, M_0 is the mass of undeuterated myoglobin from control formulations and M_{100} is the mass of myoglobin after maximum deuterium uptake corrected for back exchange. The maximum number of deuterons that can be taken up by the protein was calculated using the formula:

$$(\#\ of\ exchangeable\ amide\ hydrogens) = (\#\ of\ amino\ acids) - (\#\ of\ prolines) - 2 \quad (3)$$

and the kinetics of deuterium uptake were then fitted to a biexponential model:

$$D(\%) = D_{fast}\left(1 - e^{(-k_{fast} \times t)}\right) + D_{slow}\left(1 - e^{(-k_{slow} \times t)}\right) \quad (4)$$

where D_{fast} and D_{slow} are pre-exponential factors for two pools of amide hydrogens with fast and slow exchange rates, k_{fast} and k_{slow}. Initially, all four parameters (D_{fast}, D_{slow}, k_{fast}, k_{slow}) were considered to be functions of temperature and RH. In preliminary analyses, the biexponential model was compared to a monoexponential fit using the Akaike Information Criterion (AIC). The biexponential model showed a better fit for most data sets (not shown) and was subsequently applied to all data sets to allow comparison of regression parameters.

2.2.4. Karl Fischer titration for moisture content analysis (KF)

The moisture content of vials removed and crimped immediately after lyophilization was determined using KF coulometric titration on a Mettler Toledo C20S Coulometric KF titrator (Columbus, OH). Samples were reconstituted with 2 mL of anhydrous methanol (with sealed septum, Sigma Aldrich, St Louis, MO) to form a suspension, vortexed and allowed to stand for 3 min to ensure moisture extraction. 1 mL of the suspension was then injected into the KF assembly and titrated against Honeywell Fluka™ Hydranal Coulomat AG (Muskegon, MI) until the end point was reached. Each formulation was analyzed in triplicate.

2.2.5. Powder X-ray diffraction (PXRD)

PXRD was performed on a Rigaku SmartLab (XRD 6000) diffractometer (The Woodlands, TX) at a 0.15405 nm wavelength to assess the crystallinity of the formulations. The diffraction pattern was collected from 5° to 40° 2θ at a step size of 0.02°.

2.2.6. Solid-state FTIR

Solid-state FTIR was performed to assess the effects of various excipients on myoglobin secondary structure after lyophilization. FTIR spectra were acquired using a Nexus FTIR spectrometer (Thermo Nicolet Corp., Madison, WI). A small amount of sample was placed on the crystal and spectra were collected at a resolution of 4 cm^{-1} with 128 scans. The instrument was constantly purged with nitrogen to minimize moisture interference and was set to correct for background noise. The Amide I region was specifically extracted for each formulation and the area was normalized after baseline correction. Second derivative spectra were generated using FTIR Opus software (Bruker Optics, Billerica, MA., version 6.5).

2.2.7. Statistical analysis

Deuterium incorporation kinetics were estimated with the biexponential model (Eq. (4)) using the non-linear regression platform in JMP® Pro 15.0 (SAS Institute, Cary, NC). Several variants of the biexponential model with possible constraints on the model parameters were estimated. Details on the model fitting procedure are given in Appendix A. Models were compared and the best fit model was selected using the corrected Akaike Information Criterion (AICc). The AICc was calculated from the sum of squared errors for each model fit (SSE), the number of data points (n) and the total number of parameters in each model (q) according to the relationship (Claeskens and Hjort, 2008):

$$AICc = 2q + n\ ln(SSE) + \left(2q^2 + 2q\right)/(n - q - 1) \quad (5)$$

A smaller AICc value is indicative of a better fit.

3. Results

3.1. Solid-state FTIR

Solid-state FTIR was performed to detect differences in protein secondary structure among the lyophilized formulations. All four formulations showed a band near 1650 cm^{-1}, consistent with the native alpha helical structure of myoglobin and indicating that secondary structure is largely intact (Fig. 1(A)). A second band between 1660 and 1670 cm^{-1} also appeared in all formulations and is consistent with random coil structure. A decrease in the band intensity at 1650 cm^{-1} is indicative of a decrease in the α- helix content and was observed for dextran, mannitol and sodium chloride formulations (Alhazmi, 2019; Moorthy et al., 2014).

3.2. PXRD

PXRD was performed on fresh samples immediately after lyophilization (t = 0) and on samples incubated for 10 d at 40 °C and 43% RH. The incubation conditions were chosen to represent values of temperature, RH and incubation time in the ssHDX-MS experiments most likely to induce crystallization (i.e., high temperature, high RH, long

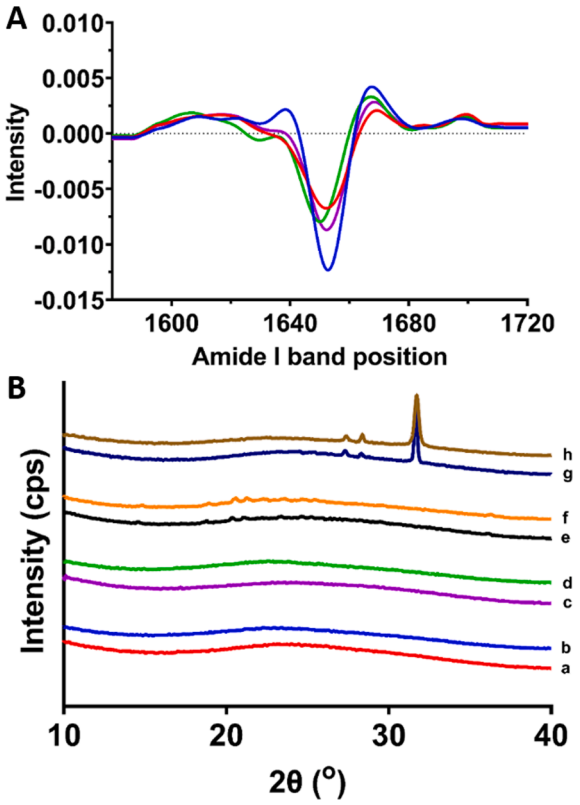

Fig. 1. (A) Solid state FTIR spectra of lyophilized myoglobin formulations containing sucrose (blue), dextran (red), mannitol (green) and sodium chloride (purple). (B) PXRD diffractograms of myoglobin formulations. (a, c, e, g) are samples evaluated after incubation at 40 °C and 43% RH for 10 d for sucrose, dextran, mannitol and sodium chloride respectively. (b, d, f, h) are samples evaluated immediately after lyophilization for sucrose, dextran, mannitol and sodium chloride formulations, respectively.

incubation time). In freshly lyophilized samples, crystallization was not observed in sucrose and dextran formulations (Fig. 1(B)). Crystallization was detected in samples containing mannitol and sodium chloride at t = 0, however, consistent with the physical properties of these excipients (Fig. 1(B)). Similarly, after 10 days of incubation, crystallization was observed in mannitol and sodium chloride formulations whereas no crystallization was observed in sucrose and dextran formulations (Fig. 1 (B)). For all formulations, the cakes had the expected appearance after lyophilization and remained solid after exposure to 40 °C and 43% RH conditions for 10 d.

3.3. ssHDX-MS

The extent of deuterium incorporation increased monotonically with time at 25 °C and 23% RH for all four formulations (Fig. 2). The results are representative of deuterium incorporation kinetics at other conditions (see Fig. S1). The rate and extent of deuterium uptake depended on both RH and temperature. For a given excipient at constant RH, the rate and extent of deuterium uptake increased with increasing temperature (Fig. 2, Fig. S1). In general, the maximum extent of deuterium incorporation (D_{max}) over the time scale of the experiment for the four formulations increased in the order: sucrose < dextran < mannitol < sodium chloride (Fig. 2, Fig. S1), though differences among the formulations varied with experimental conditions. Formulations containing mannitol or sodium chloride showed consistently greater deuterium uptake than sucrose and dextran formulations. Since myoglobin secondary structure is largely retained in all four formulations (Fig. 1A), this suggests that sucrose and dextran interact with the protein in ways that protect it from exchange, probably through the formation of

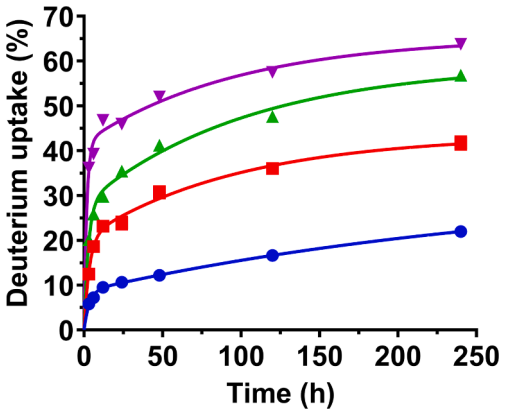

Fig. 2. Deuterium uptake as a function of time for lyophilized myoglobin formulations containing sucrose (blue), dextran (red), mannitol (green) or sodium chloride (purple) as excipients at 25 °C and 23% RH. Deuterium uptake is expressed as percent of theoretical maximum. N = 3 ± SD. Error bars not shown when smaller than the symbol.

intermolecular hydrogen bonds. Greater deuterium incorporation in sodium chloride and mannitol formulations suggests that such interactions are weaker or absent with these excipients. Chemical structure and partial crystallinity of sodium chloride and mannitol (Fig. 1) may limit their interactions with myoglobin. KF moisture analysis was performed after lyophilization to determine the residual moisture content of the samples. Sucrose, dextran, mannitol and sodium chloride showed moisture values of 0.69 ± 0.06%, 0.63 ± 0.10%, 0.64 ± 0.15% and 0.99 ± 0.05% respectively (Table S7). This suggests that differences in initial moisture content are unlike to contribute appreciably to differences in the rate and extent of ssHDX-MS.

Deuterium incorporation kinetics were fitted to a biexponential equation (Eqn. (4)) to generate the regression parameters (D_{fast}, D_{slow}, k_{fast}, k_{slow}). The greater of the two rate constants was designated k_{fast} and the corresponding D value was designated D_{fast}. The optimal parameters for each deuterium incorporation profile were determined by analyzing the data for each lyophilized formulation and condition (i.e., RH, T) separately using the non-linear regression platform in JMP® Pro 15.0. This model was called Model I.

The parameter estimates were plotted against RH and temperature for all four formulations and linear regression analyses were performed. The dependence of each parameter estimate on RH and on temperature was determined by comparing the slopes of the lines to 0 at $p < 0.1$. With the exception of the sodium chloride formulation, all formulations showed nonzero slopes for D_{fast} versus RH at all temperatures studied ($p < 0.1$) (Fig. 3). Sodium chloride formulations did not show a nonzero slope of D_{fast} versus RH at any temperature. In contrast, D_{slow} values did not show a dependence on RH at any temperature for any formulation. With regard to the rate constants, k_{fast} showed no dependence on RH for any excipient at any temperature, with the exceptions of dextran at 40 °C and mannitol at 25 °C. Similarly, k_{slow} values showed a dependence on RH only for sucrose at 40 °C (Fig. 4).

The dependences of the parameter values on temperature were also explored. A dependence of D_{fast} on temperature was observed for sucrose at 11%, 23% and 43% RH and for dextran at 6%, 11% and 43% RH (Fig. 5). D_{fast} for mannitol showed a temperature dependence at all RH values, while sodium chloride showed no dependence of D_{fast} on temperature at any RH value (Fig. 5). D_{slow} was affected by temperature for sucrose and dextran at 6% RH and for mannitol at 23% RH; other conditions showed no dependence of D_{slow} on temperature (Fig. 5). The k_{fast} values were significantly affected by temperature for sucrose, dextran and mannitol at 43% RH (Fig. 6), while k_{slow} did not show any dependence on temperature for any of the formulations.

In addition to evaluating the effects of RH and temperature singly, a

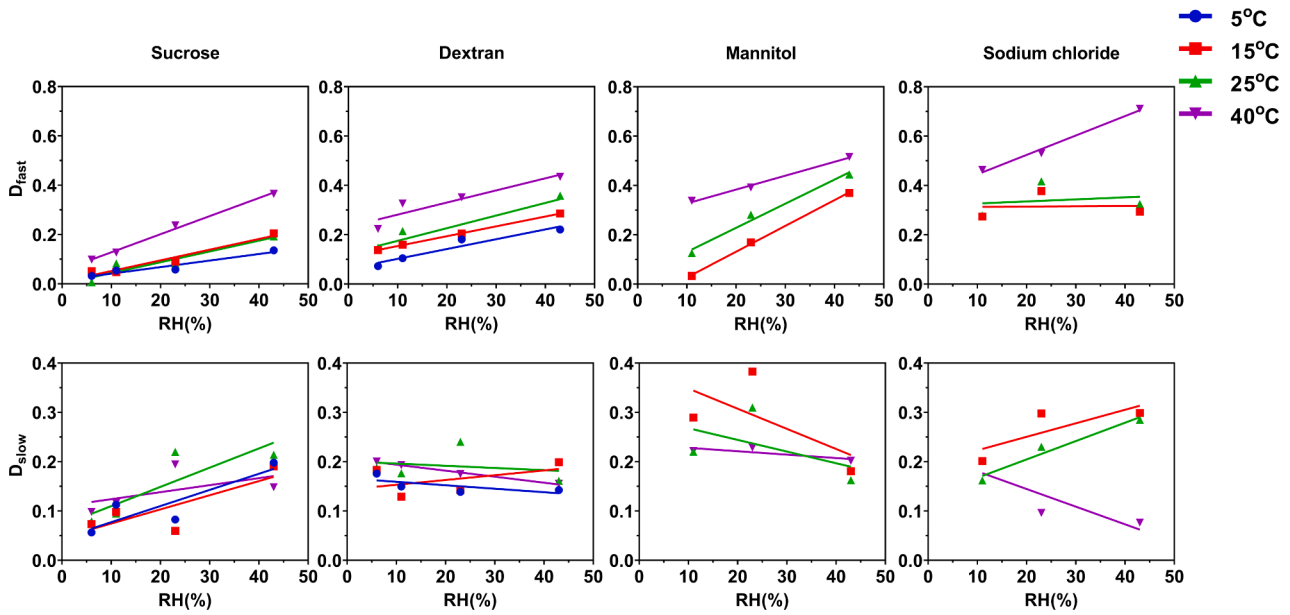

Fig. 3. D_{fast} and D_{slow} values (Model I) as a function of RH and temperature (5 °C = blue, 15 °C = red, 25 °C = green, 40 °C = purple) for myoglobin formulations containing sucrose, dextran, mannitol or sodium chloride.

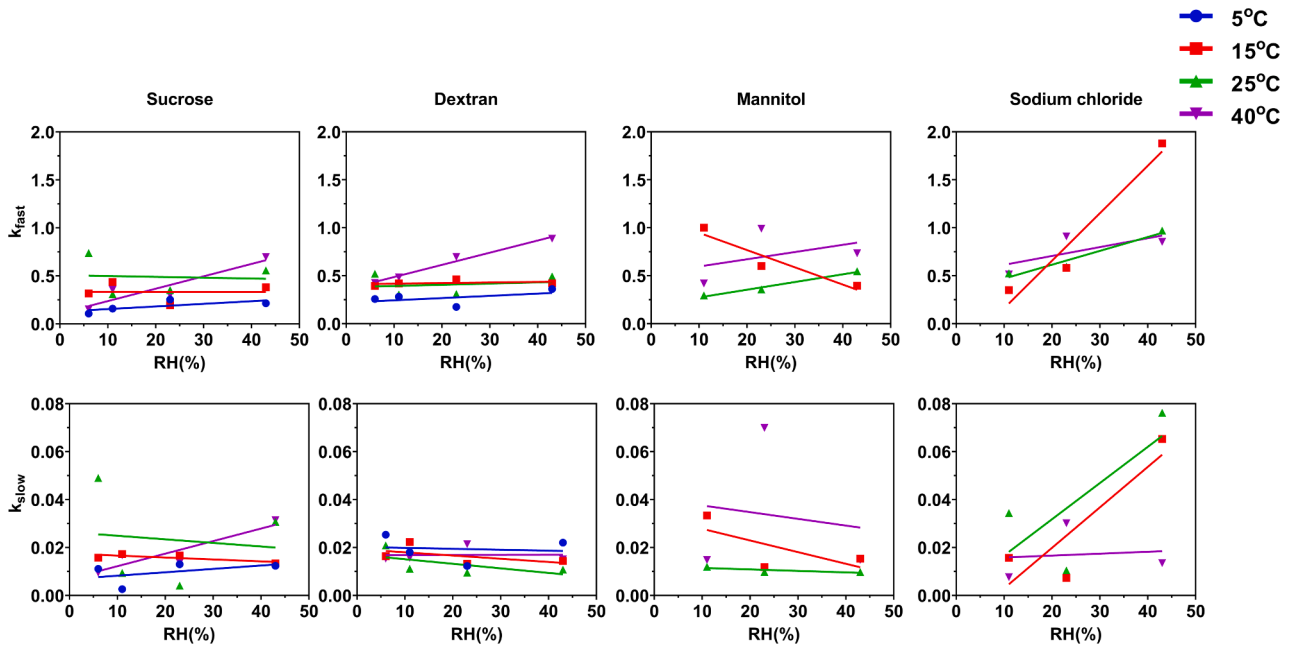

Fig. 4. k_{fast} and k_{slow} rate constants (Model I) as a function of RH and temperature (5 °C = blue, 15 °C = red, 25 °C = green, 40 °C = purple) for myoglobin formulations containing sucrose, dextran, mannitol or sodium chloride.

response surface model (RSM) was constructed to explore possible interactions between RH and temperature on the parameter values (Gunst et al., 1996) (Table S1). Model terms with $p < 0.1$ were considered significant and retained in the RSM. For sucrose, D_{fast} showed a significant dependence on both RH and on temperature, and an interaction between the two, while k_{fast} showed a dependence on temperature alone. For dextran, D_{fast} showed a dependence on RH and temperature, and k_{fast} showed a dependence on temperature and an interaction between RH and temperature. Mannitol and sodium chloride D_{fast} values showed a dependence on RH, temperature and an interaction between the two, while sodium chloride k_{fast} values showed a dependence on RH. D_{slow} for sucrose and mannitol showed RH dependence. k_{slow} values for sodium chloride showed a dependence on $(RH)^2$ and $(temperature)^2$, the quadratic relation being representative of a curvilinear relationship rather than a linear relationship (Table S1).

In summary, statistical analysis using JMP® Pro demonstrated that D_{fast} shows a significant dependence on both temperature and RH for all four formulations studied (Table S1). The rate constant k_{fast} shows a significant dependence on temperature for two of the four formulations, and on RH for one of the four formulations (Table S1). In contrast, D_{slow} shows a significant dependence on RH for only one of the four formulations and is independent of temperature for all four formulations (Table S1). Similarly, k_{slow} is independent of both temperature and RH for three of the four formulations (Table S1). This suggests that the temperature and RH dependences of the biexponential model can be simplified by assuming that k_{slow} and/or D_{slow} are independent of

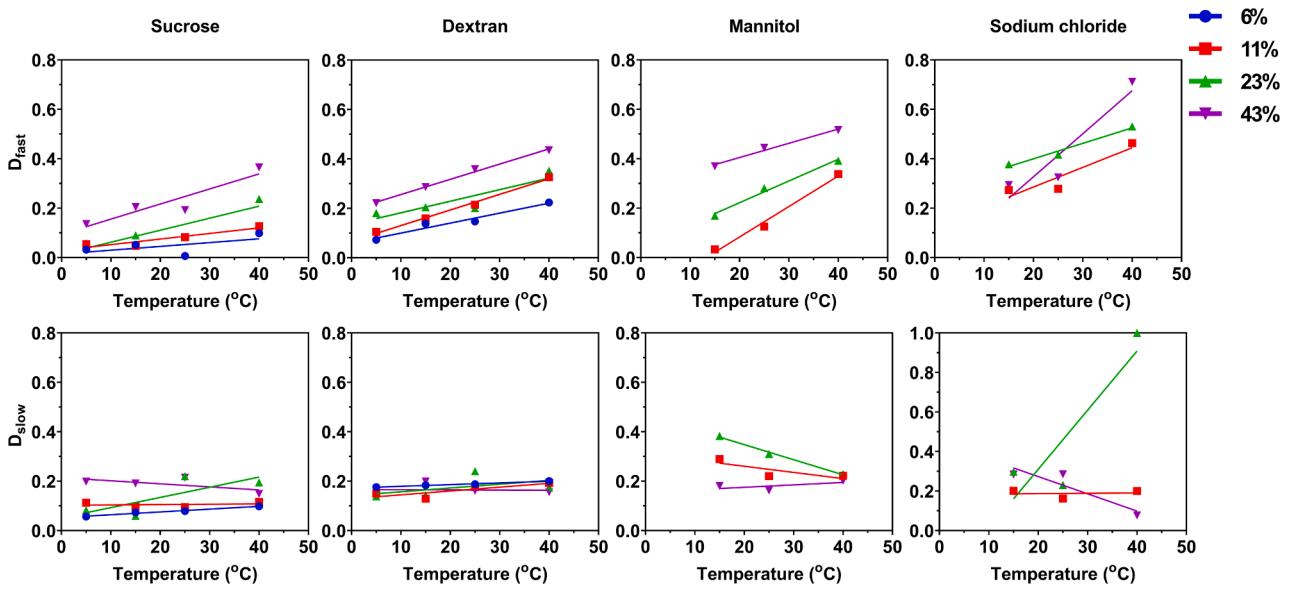

Fig. 5. D_{fast} and D_{slow} values (Model I) as a function of temperature and RH (6% = blue, 11% = red, 23% = green, 43% = purple) for myoglobin formulations containing sucrose, dextran, mannitol or sodium chloride.

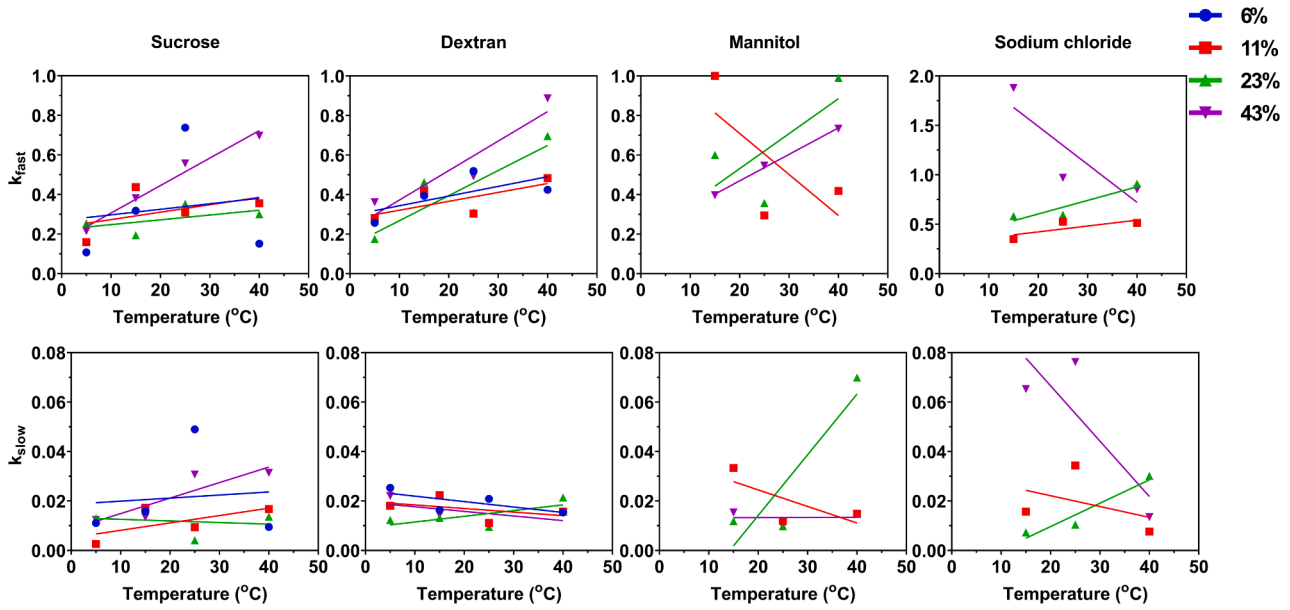

Fig. 6. k_{fast} and k_{slow} rate constants (Model I) as a function of temperature and RH (6% = blue, 11% = red, 23% = green, 43% = purple) for myoglobin formulations containing sucrose, dextran, mannitol or sodium chloride.

temperature and RH, providing greater statistical power in estimating these dependences for D_{fast} and k_{fast}. This model simplification is described below.

3.4. Reducing the models

The graphical and RSM analysis of the unconstrained Model I fits showed a lack of consistent trends in the parameter estimates with respect to RH and temperature. The weak dependences of D_{slow} and k_{slow} on temperature and RH suggest that the model can be simplified by holding one or both of these parameters invariant with temperature and RH. Therefore, a constrained version of the biexponential model, labeled Model II, in which the slow rate parameter (k_{slow}) was invariant with RH and temperature (i.e., $k_{slow} \neq f(T, RH)$) was fit to the data (see Appendix A).

The relationships between the regression parameters in Model II and RH or temperature are shown in Figs. S2–S5. The results of the response surface analysis on this model are summarized in Table S2. While D_{fast} did show a dependence on RH generally in Model II, for sucrose this relationship was curvilinear (Fig. S2). Similarly, D_{fast} values showed a curvilinear dependence on temperature for all excipients (Fig. S4). The curvature indicates a co-dependence of RH and temperature, or an RH^2 and/or $temperature^2$ dependence (see Table S2). k_{fast} values showed a curvilinear dependence on RH (Fig. S3) and generally increased with temperature (Fig. S5) in Model II.

The model was further simplified (Model III) to hold both D_{slow} and k_{slow} invariant with RH and temperature (D_{slow}, $k_{slow} \neq f(T, RH)$) while the parameters k_{fast} and D_{fast} were allowed to vary with temperature and RH. As with Model II, a response surface analysis was generated to show any interactions between RH and temperature for k_{fast} and D_{fast} in the

various formulations. In Model III, D_{fast} generally increased with RH for sucrose, dextran and sodium chloride formulations, but showed an initial increase followed by a plateau for the mannitol formulation (Fig. S6). D_{fast} increased monotonically with temperature for all four formulations in Model III (Fig. S8). In Model III, k_{fast} values increased with RH and temperature for most formulations but decreased with both RH and temperature for sucrose formulations at low temperature and at low RH (Fig. S7, S9). The response surface analyses for Model III are summarized in Table S3.

The model was further reduced to the case in which only D_{fast} was allowed to vary with temperature and RH and (D_{slow}, k_{fast}, k_{slow}) were invariant with RH and temperature (Model IV). The model with the best overall fit to the data was selected based on the AICc values (see Section 2.2.6, Fig. 7). Model III showed the lowest AICc values for the dextran, mannitol and sodium chloride formulations, indicating the best fit for these formulations (Fig. 7). In contrast, the sucrose formulation showed the lowest AICc value for Model II (Fig. 7). Model IV gave AICc values comparable to those of Model III for the sucrose, mannitol and sodium chloride formulations, but poorer values for the dextran formulation (Fig. 7). Based on these results, and for the sake of consistency, Model III was selected for all formulations, and corresponds to the simplification in which the slow rate process (D_{slow}, k_{slow}) is assumed to be invariant with temperature and RH.

Fig. 8 summarizes the RH and temperature dependences of k_{fast} for the four formulations for Model III as contour plots. The contour plots for k_{fast} in the sucrose and mannitol formulations indicate that k_{fast} depends on both temperature and RH (Fig. 8A, C). In contrast, k_{fast} in the dextran formulation shows a dependence on RH and temperature, as well as an interaction effect. While k_{fast} in the sodium chloride formulation shows contours similar to those observed for dextran, there is a somewhat greater sensitivity to changes in temperature at low RH values, and to RH at low temperature values.

Fig. 9 shows the corresponding D_{fast} contour plots for Model III. The D_{fast} values for the sucrose formulation show a strong dependence on temperature and RH, as well as an interaction between the two (Fig. 9A). D_{fast} values for dextran, mannitol and sodium chloride also depend on both temperature and RH, but there is no temperature-RH interaction (Fig. 9B–D). The contour lines are the most closely spaced for sodium chloride followed by mannitol and then dextran. These differences in contour line spacing indicate that, for a given change in temperature or RH, the D_{fast} values show the greatest changes for sodium chloride with smaller changes for mannitol and the least change for dextran.

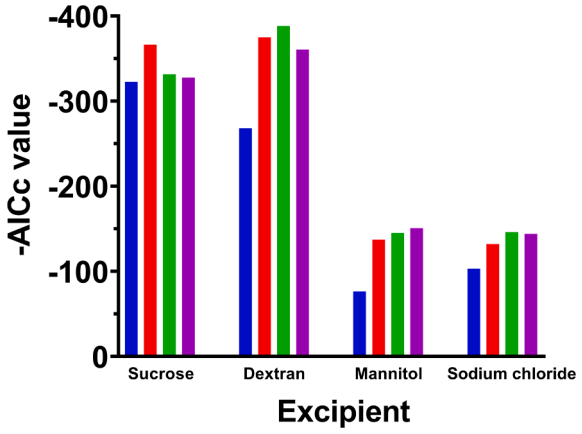

Fig. 7. Comparison of AICc values of Model I (blue), Model II (red), Model III (green) and Model IV (purple) for the four myoglobin formulations containing either sucrose, dextran, mannitol or sodium chloride. Model I is the full bi-exponential model, Model II is the model where $k_{slow} \neq f(T, RH)$, Model III is the model where D_{slow}, $k_{slow} \neq f(T, RH)$, Model IV has D_{slow}, k_{slow}, $k_{fast} \neq f(T, RH)$. Note: The vertical axis represents negative AICc (-AICc) values.

4. Discussion

In the studies presented here, myoglobin formulations with similar residual moisture content after lyophilization were exposed to $D_2O(g)$ at a range of temperature and RH conditions, and the resulting deuterium uptake kinetics were fitted to a biexponential model using nonlinear regression. The dependences of the regression parameters (i.e., D_{fast}, k_{fast}, D_{slow}, k_{slow}) on temperature and RH were then evaluated. Overall, the best fit to the data set was provided by a simplified model (Model III) in which D_{slow} and k_{slow} were considered invariant with temperature and RH while D_{fast} and k_{fast} retained their temperature and RH dependence. A simple explanation for the effectiveness of Model III may be that the fast exponential term makes a greater contribution to the total deuterium uptake than the slow exponential term, so that the temperature and RH dependence of deuterium incorporation can be lumped into the fast term with little loss in goodness of fit. To test this explanation, the contributions of the fast and slow exponential terms (Eqn. (4)) to the deuterium uptake were calculated for each time point of each data set, using the regression parameters for Model I. The combined data set consists of 350 time points in 50 experiments, which differ in the type of excipient and in the temperature and RH of deuterium exposure (Table S5). In 228 of the 350 time points (~65%), the fast exponential term contributed at least 70% of the total value of deuterium uptake (D) calculated using Model I (Table S5). In general, the contribution of the fast exponential term was greatest at short times and at higher RH and temperature values (Table S5). At later time points, the contribution of the fast phase to the total deuterium content plateaued while the contribution of the slow phase continued to increase. Thus, it is possible to attribute the RH and temperature dependences of deuterium incorporation to the fast exponential term alone (D_{fast}, k_{fast}) because this term makes the greatest contribution to the calculated deuterium incorporation (D) for most of the time points in the studies conducted here.

An alternative explanation for the observed RH and temperature dependence of the fast phase is more mechanistic. In previous ssHDX-MS studies using unstructured PDLA peptides, we have shown that deuterium incorporation kinetics can be described by a reversible first-order model, in which the forward rate constant is proportional to $D_2O(g)$ activity (i.e., RH in D_2O) (Kammari and Topp, 2019). We have also shown that the initial sorption of $H_2O(g)$ in ssHDX-MS occurs rapidly, and typically is complete in 1–2 h (Sophocleous et al., 2012; Sophocleous and Topp, 2012). These findings suggest that, in the studies of myoglobin reported here, the observed RH dependence of the fast phase may reflect the RH-dependent processes of $D_2O(g)$ sorption into the solid and the initial forward exchange reaction. It is reasonable to expect that these processes also depend on temperature, since water vapor sorption and therefore the forward rate of deuteration in solution HDX (i.e., the rate of chemical exchange) are both known to be temperature dependent (Gallagher and Hudgens, 2016; Grant et al., 1999; Umprayn and Mendes, 1987). Thus, the RH and temperature dependences of the fast phase of myoglobin deuteration may reflect the RH and temperature dependences of $D_2O(g)$ sorption and the initial forward exchange reaction. In contrast, the slow phase of myoglobin ssHDX was relatively independent of RH and temperature (Model III). In the previous studies of unstructured PDLA peptides noted above, ssHDX-MS kinetics were consistent with a reverse reaction (loss of deuterium) that was independent of RH (Kammari and Topp, 2019). This suggests that, in the studies reported here, the slow phase of myoglobin deuteration may involve RH-independent loss of deuteration from initial sites of labeling, followed by deuteration at nearby amide groups. Like other reactions, these processes are expected to depend on temperature, but the extent of this dependence is not known. Thus, the weak RH dependence of the slow phase of myoglobin deuteration may reflect the weak RH dependence of the reverse reaction and transfer of label through the matrix, followed by the slow but steady increase in deuterium uptake by more protected regions of the protein molecule.

The results of the studies have implications for how ssHDX-MS

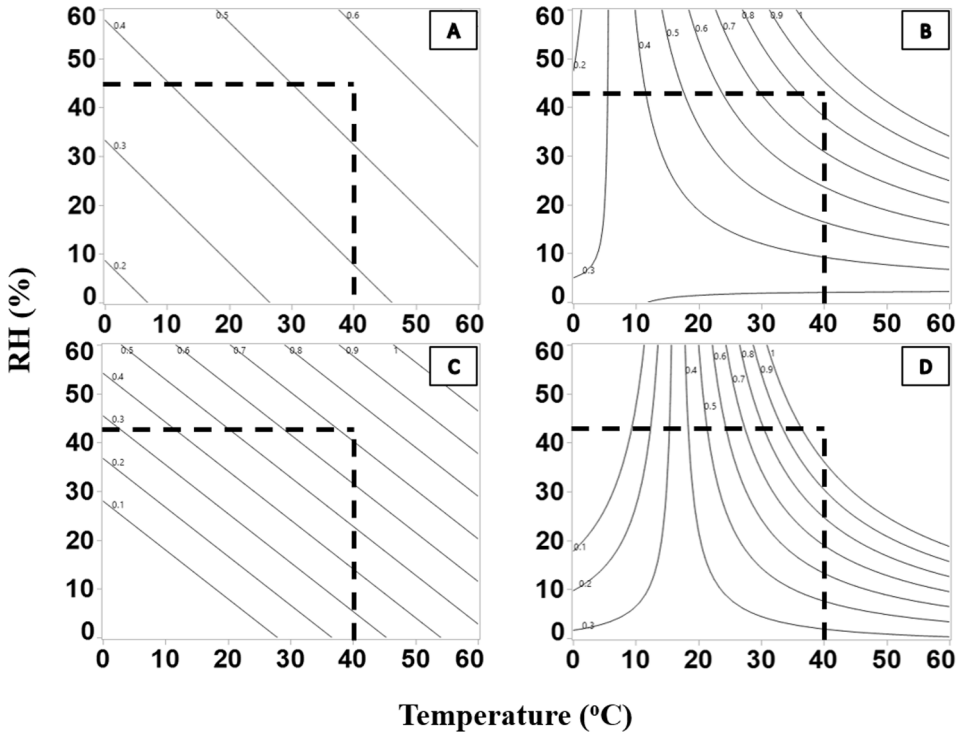

Fig. 8. Contour plots for k_{fast} for (A) sucrose, (B) dextran, (C) mannitol, (D) sodium chloride Model III (D_{slow}, $k_{slow} \neq f(T, RH)$). The dotted lines represent boundaries of experimental conditions studied.

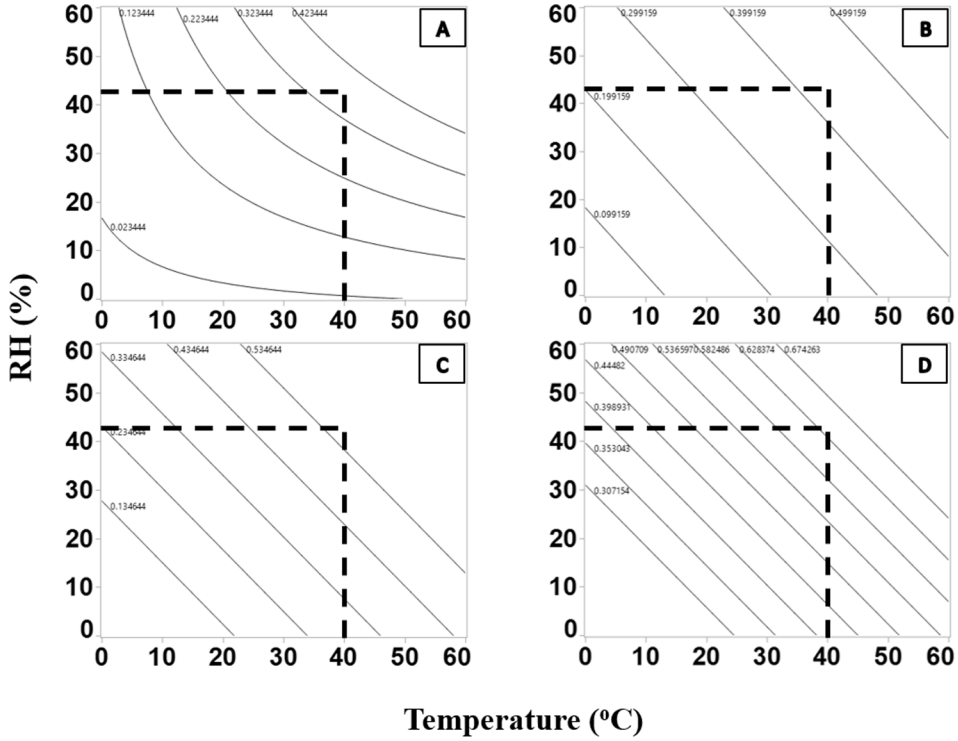

Fig. 9. Contour plots for D_{fast} for (A) sucrose, (B) dextran, (C) mannitol, (D) sodium chloride Model III (D_{slow}, $k_{slow} \neq f(T, RH)$). The dotted lines represent boundaries of experimental conditions studied.

experiments are performed. In particular, the results suggest that judicious choice of temperature and RH conditions can improve the information obtained from an ssHDX-MS experiment. Here, the greatest separation between deuterium incorporation curves for different formulations was observed at 23% RH and 25 °C (Fig. S1 and Fig. 2). Increasing or decreasing the temperature or RH reduced the separation between the curves, and at extreme conditions (i.e., very low or very high RH or temperatures) resolution was lost (Fig. S1). At 23% RH and 25 °C, the deuterium incorporation curves were separated by a minimum of 6% to a maximum of 20% deuterium uptake. On the other hand,

at 43% RH and 40 °C, separation ranged from 1% to 14% (Fig. S1). Therefore, for myoglobin, the 23%RH and 25 °C experimental conditions provided maximum information on differences among the formulations. Furthermore, at these conditions, the maximum separation between the curves was achieved by 48 h of deuterium incorporation (Fig. 2). Extending the experiment to longer sampling times did not notably increase the separation, although additional time points might improve the fit for regression parameters of the slow phase (D_{slow}, k_{slow}). This suggests that rate processes associated with the fast phase of deuterium incorporation, as discussed above, are primarily responsible for the differences in the formulations studied here. Thus, for myoglobin samples, ssHDX-MS can provide information about differences among formulations using incubation at 23 %RH and 25 °C and a single incubation time point at 2 to 7 days. Although the optimum deuteration conditions and incubation time may vary with protein and sample type (e.g., fill volume), they could be established in screening studies like those reported here, improving overall ssHDX-MS workflow.

5. Conclusions

Lyophilized myoglobin formulations with various excipients were subjected to ssHDX-MS at different temperatures and RH values. Deuterium incorporation kinetics was then fitted to a bi-exponential model and the dependences of regression parameters on temperature and RH were analyzed statistically. The best fit was provided by a simplified model in which parameters for the slow exponential term (D_{slow}, k_{slow}) were independent of temperature and RH. The results suggest that relatively fast rate processes, such as D_2O sorption and initial amide deuteration, depend on temperature and RH and are primarily responsible for differences among formulations. The results also suggest that optimum deuteration conditions and single-point sampling times can be identified for a particular protein and sample type, streamlining ssHDX-MS workflow.

CRediT authorship contribution statement

Rishabh Tukra: Investigation, Formal analysis, Writing - original draft, Visualization. **Sam Gardner:** Methodology, Formal analysis, Writing - original draft. **Elizabeth M. Topp:** Conceptualization, Supervision, Writing - review & editing.

Declaration of Competing Interest

The authors declare that they have no known competing financial interests or personal relationships that could have appeared to influence the work reported in this paper.

Acknowledgements

Lyophilization assistance was provided by the LyoHUB Core Facility at Purdue University. The authors also thank Dr. Karthik Balakrishna Chandrababu for assistance with FTIR.

This research did not receive any specific grant from funding agencies in the public, commercial, or not-for-profit sectors.

Appendix A

This work applies several types of statistical approaches for the study design and data analysis. As these methods may not be familiar to the reader, they are described in more detail below.

Design of Experiments (DOE)

Statistical Design of Experiments (DOE) is an efficient approach to experimentation that allows for the discovery of the relationships between experimental factors and the observed outputs of the experimental system. In this study, full factorial (FF) designs were employed as described in the body of the paper. A full factorial design is constructed by determining every combination of the experimental factor levels and conducting the experiments at all those combinations. The FF designs (for the temperature and relative humidity factors) used in this study allow for the estimation of polynomial regression relationships, with interactions, between those factors and the observed ssHDX results. Those relationships are estimated using standard linear regression methods that are available in many statistical analysis software tools.

Functional Data Analysis using Non-Linear Regression

The primary experimental "observation" for each combination of temperature and humidity is a profile of the HDX results vs time, with seven time points for each profile. This type of data is also known as "functional data", in that the measured results can be thought of as profile of results which are a function of time. The experimenter is faced with a challenge on how to correlate the experimental factors (temperature and relative humidity) with the functional response.

A common approach in this situation is to assume that an underlying parameterized function of time describes the experimental profile, and to estimate the parameters for that function for each profile. The experimenter than uses those estimated functional parameters as the "data" for the experiment. This approach has two benefits: 1) it serves to reduce the data from a profile with many points to a smaller set of functional parameters; and 2) if the model functional parameters can be assigned a physical meaning that explains the underlying mechanics of the system being observed, then correlating the experimental factors with the functional parameters can lead to a better understanding of the underlying process that is generating the experimental results.

Functional data analysis for this study in performed using non-linear regression. The functional models used are non-linear in the model parameters and standard linear regression approaches cannot be used to estimate those model parameters. In the function form for each profile is assumed to follow a form of the bi-exponential model

$$D(t) = D_{\text{fast}}\left(1 - e^{-k_{\text{fast}}t}\right) + D_{\text{slow}}\left(1 - e^{-k_{\text{slow}}t}\right) \tag{A.1}$$

Defining the profile as the collection of responses (ssHDX) $\{Y(t_1), Y(t_1), \cdots, Y(t_{N_t})\}$ are made at time points $\{t_1, t_2, \cdots, t_{N_t}\}$, then the model parameters that provide the best fit to the profile are those that minimize the sum of squared errors (SSE) between the data and the model.

$$SSE = \sum_{z=1}^{N_t} \left(D(t_z) - Y(t_z)\right)^2 \tag{A.2}$$

This approach converts the profile data $\{\{Y(t_1), Y(t_1), \cdots, Y(t_{N_t})\}, \{t_1, t_2, \cdots, t_{N_t}\}\}$ to a set of estimated model parameters $\{D_{\text{fast}}, D_{\text{slow}}, -k_{\text{fast}}, -k_{\text{slow}}\}$.

Applying nonlinear regression to full and reduced models

This estimation approach was extended so that several types of non-linear models of varying complexity could be estimated efficiently and compared against each other. The approach allowed for simultaneous estimation of all model parameters for all profiles (for a given excipient), as well as allowing certain parameters to be constrained to be the same across all profiles. The general approach used was to index each profile according to the experimental conditions and create a combined SSE for the combined profiles generated across all experimental conditions.

More explicitly, we let the experimental factors be represented by

$\{T_1, T_2, \cdots, T_{N_T}\}$ (for temperature) and

$\{RH_1, RH_2, \cdots, RH_{N_{RH}}\}$(for relative humidity).

We define the nonlinear model for the collection of functional data be

$$D(t_z)_{T_x,RH_y} = D_{\text{fast},T_x,RH_y}\left(1 - e^{-k_{\text{fast},T_x,RH_y}t_z}\right) + D_{\text{slow},T_x,RH_y}\left(1 - e^{-k_{\text{slow},T_x,RH_y}t_z}\right) \tag{A.3}$$

Letting the profile data generated for each for each combination of (T_x, RH_y) be represented as

$$\left\{\left(Y_{T_x,RH_y}(t_z), t_z\right) : z = 1, \cdots, N_t\right\}$$

then the combined SSE

$$SSE = \sum_{x=1}^{N_T}\sum_{y=1}^{N_{RH}}\sum_{z=1}^{N_t}\left(D(t_z)_{T_x,RH_y} - Y_{T_x,RH_y}(t_z)\right)^2 \tag{A.4}$$

is used at the objective function in the non-linear estimation algorithm. The results in simultaneous estimation of all the model parameters $\{D_{\text{fast},T_x,RH_y}, D_{\text{slow},T_x,RH_y}, k_{\text{fast},T_x,RH_y}, k_{\text{slow},T_x,RH_y}\}$ that correspond to the profile for each experimental condition (T_x, RH_y).

Reduced models were estimated by setting specific parameters to be the same across all profiles. The common slow rate model uses the substitution $k_{\text{slow},T_x,RH_y} \equiv k_{slow}$ so that

$$D(t_z)_{T_x,RH_y} = D_{\text{fast},T_x,RH_y}\left(1 - e^{-k_{\text{fast},T_x,RH_y}t_z}\right) + D_{\text{slow},T_x,RH_y}\left(1 - e^{-k_{\text{slow}}t_z}\right) \tag{A.5}$$

The common slow process model uses the substitutions $k_{\text{slow},T_x,RH_y} \equiv k_{slow}$ and $D_{\text{slow},T_x,RH_y} \equiv D_{slow}$ so that

$$D(t_z)_{T_x,RH_y} = D_{\text{fast},T_x,RH_y}\left(1 - e^{-k_{\text{fast},T_x,RH_y}t_z}\right) + D_{\text{slow}}\left(1 - e^{-k_{\text{slow}}t_z}\right) \tag{A.6}$$

Appendix B. Supplementary material

Supplementary data to this article can be found online at https://doi.org/10.1016/j.ijpharm.2021.120263.

References

Alhazmi, H.A., 2019. FT-IR spectroscopy for the identification of binding sites and measurements of the binding interactions of important metal ions with bovine serum albumin. Sci. Pharm. 87 https://doi.org/10.3390/scipharm87010005.

Allison, S.D., Manning, M.C., Randolph, T.W., Middleton, K., Davis, A., Carpenter, J.F., 2000. Optimization of storage stability of lyophilized actin using combinations of disaccharides and dextran. J. Pharm. Sci. 89, 199–214. https://doi.org/10.1002/(SICI)1520-6017(200002)89:2<199::AID-JPS7>3.0.CO;2-B.

Claeskens, G., Hjort, N.L., 2008. Model Selection and Model Averaging. Model Selection and Model Averaging. Cambridge University Press. https://doi.org/10.1017/CBO9780511790485.

Fang, R., Grobelny, P.J., Bogner, R.H., Pikal, M.J., 2016. Protein internal dynamics associated with pre-system glass transition temperature endothermic events: investigation of insulin and human growth hormone by solid state hydrogen/deuterium exchange. J. Pharm. Sci. 105, 3290–3295. https://doi.org/10.1016/j.xphs.2016.07.028.

Gallagher, E.S., Hudgens, J.W., 2016. Mapping protein-ligand interactions with proteolytic fragmentation, hydrogen/deuterium exchange-mass spectrometry. In: Methods in Enzymology. Academic Press Inc., pp. 357–404. https://doi.org/10.1016/bs.mie.2015.08.010

Grant, A., Belton, P.S., Colquhoun, I.J., Parker, M.L., Plijter, J.J., Shewry, P.R., Tatham, A.S., Wellner, N., 1999. Effects of temperature on sorption of water by wheat gluten determined using deuterium nuclear magnetic resonance. Cereal Chem. 76, 219–226. https://doi.org/10.1094/CCHEM.1999.76.2.219.

Gunst, R.F., Myers, R.H., Montgomery, D.C., 1996. Response surface methodology: process and product optimization using designed experiments. Technometrics 38, 285. https://doi.org/10.2307/1270613.

Horn, J., Friess, W., 2018. Detection of collapse and crystallization of saccharide, protein, and mannitol formulations by optical fibers in lyophilization. Front. Chem. 6 https://doi.org/10.3389/fchem.2018.00004.

Hvidt, A., Linderstrøm-Lang, K., 1955. The kinetics of the deuterium exchange of insulin with D2O. An amendment. BBA - Biochim. Biophys. Acta 16, 168–169. https://doi.org/10.1016/0006-3002(55)90200-6.

Hvidt, A., Linderstrøm-Lang, K., 1954. Exchange of hydrogen atoms in insulin with deuterium atoms in aqueous solutions. BBA - Biochim. Biophys. Acta 14, 574–575. https://doi.org/10.1016/0006-3002(54)90241-3.

Iyer, L.K., Sacha, G.A., Moorthy, B.S., Nail, S.L., Topp, E.M., 2016. Process and formulation effects on protein structure in lyophilized solids using mass spectrometric methods. J. Pharm. Sci. 105, 1684–1692. https://doi.org/10.1016/J.XPHS.2016.02.033.

Kabaria, S.R., Mangion, I., Makarov, A.A., Pirrone, G.F., 2019. Use of MALDI-MS with solid-state hydrogen deuterium exchange for semi-automated assessment of peptide and protein physical stability in lyophilized solids. Anal. Chim. Acta 1054, 114–121. https://doi.org/10.1016/j.aca.2018.12.034.

Kammari, R., Topp, E.M., 2019. Solid-state hydrogen-deuterium exchange mass spectrometry (ssHDX-MS) of lyophilized poly-D, L-alanine. Mol. Pharm. 16, 2935–2946. https://doi.org/10.1021/acs.molpharmaceut.9b00162.

Kulkarni, S.S., Suryanarayanan, R., Rinella, J.V., Bogner, R.H., 2018. Mechanisms by which crystalline mannitol improves the reconstitution time of high concentration lyophilized protein formulations. Eur. J. Pharm. Biopharm. 131, 70–81. https://doi.org/10.1016/j.ejpb.2018.07.022.

Larsen, B.S., Skytte, J., Svagan, A.J., Meng-Lund, H., Grohganz, H., Löbmann, K., 2019. Using dextran of different molecular weights to achieve faster freeze-drying and improved storage stability of lactate dehydrogenase. Pharm. Dev. Technol. 24, 323–328. https://doi.org/10.1080/10837450.2018.1479866.

Li, Y., Williams, T.D., Schowen, R.L., Topp, E.M., 2007. Characterizing protein structure in amorphous solids using hydrogen/deuterium exchange with mass spectrometry. Anal. Biochem. 366, 18–28. https://doi.org/10.1016/j.ab.2007.03.041.

Li, Y., Williams, T.D., Topp, E.M., 2008. Effects of excipients on protein conformation in lyophilized solids by hydrogen/deuterium exchange mass spectrometry. Pharm. Res. 25, 259–267. https://doi.org/10.1007/s11095-007-9365-6.

Lonardo, A.J., Srivastava, A., Singh, S., Goldstein, J., 2012. Robustness index score: a new stability parameter for designing robustness into biologic formulations. J. Pharm. Sci. https://doi.org/10.1002/jps.22776.

Lu, X., Pikal, M.J., 2004. Freeze-drying of mannitol–trehalose–sodium chloride-based formulations: the impact of annealing on dry layer resistance to mass transfer and cake structure. Pharm. Dev. Technol. 9, 85–95. https://doi.org/10.1081/PDT-120027421.

Moorthy, B., Iyer, L., Topp, E., 2015a. Characterizing Protein Structure, Dynamics and Conformation in Lyophilized Solids. Curr. Pharm. Des. 21, 5845–5853. https://doi.org/10.2174/1381612821666151008150735.

Moorthy, B.S., Ghomi, H.T., Lill, M.A., Topp, E.M., 2015b. Structural transitions and interactions in the early stages of human glucagon amyloid fibrillation. Biophys. J. 108, 937–948. https://doi.org/10.1016/j.bpj.2015.01.004.

Moorthy, B.S., Iyer, L.K., Topp, E.M., 2015c. Mass spectrometric approaches to study protein structure and interactions in lyophilized powders. J. Vis. Exp., 52503 https://doi.org/10.3791/52503.

Moorthy, B.S., Schultz, S.G., Kim, S.G., Topp, E.M., 2014. Predicting protein aggregation during storage in lyophilized solids using solid state amide hydrogen/deuterium exchange with mass spectrometric analysis (ssHDX-MS). Mol. Pharm. 11, 1869–1879. https://doi.org/10.1021/mp500005v.

Moorthy, B.S., Xie, B., Panchal, J.P., Topp, E.M., 2016. Hydrogen Exchange mass spectrometry for proteins adsorbed to solid surfaces, in frozen solutions, and in amorphous solids. In: Hydrogen Exchange Mass Spectrometry of Proteins. John Wiley & Sons, Ltd, Chichester, UK, pp. 265–277. https://doi.org/10.1002/9781118703748.ch15.

Moorthy, B.S., Zarraga, I.E., Kumar, L., Walters, B.T., Goldbach, P., Topp, E.M., Allmendinger, A., 2018. Solid-state hydrogen-deuterium exchange mass spectrometry: correlation of deuterium uptake and long-term stability of lyophilized monoclonal antibody formulations. Mol. Pharm. 15, 1–11. https://doi.org/10.1021/acs.molpharmaceut.7b00504.

Moroco, J.A., Engen, J.R., 2015. Replication in bioanalytical studies with HDX MS: aim as high as possible. Bioanalysis 7, 1065–1067. https://doi.org/10.4155/bio.15.46.

Moussa, E.M., Singh, S.K., Kimmel, M., Nema, S., Topp, E.M., 2018. Probing the conformation of an IgG1 monoclonal antibody in lyophilized solids using solid-state hydrogen-deuterium exchange with mass spectrometric analysis (ssHDX-MS). Mol. Pharm. 15, 356–368. https://doi.org/10.1021/acs.molpharmaceut.7b00696.

Rauk, A.P., Guo, K., Hu, Y., Cahya, S., Weiss, W.F., 2014. Arrhenius time-scaled least squares: a simple, robust approach to accelerated stability data analysis for bioproducts. J. Pharm. Sci. 103, 2278–2286. https://doi.org/10.1002/jps.24063.

Sophocleous, A.M., Topp, E.M., 2012. Localized hydration in lyophilized myoglobin by hydrogen-deuterium exchange mass spectrometry. 2. Exchange kinetics. Mol. Pharm. 9, 727–733. https://doi.org/10.1021/mp2004093.

Sophocleous, A.M., Zhang, J., Topp, E.M., 2012. Localized hydration in lyophilized myoglobin by hydrogen-deuterium exchange mass spectrometry. 1 Exchange mapping. Mol. Pharm. 9, 718–726. https://doi.org/10.1021/mp3000088.

Umprayn, K., Mendes, R.W., 1987. Hygroscopicity and moisture adsorption kinetics of pharmaceutical solids: a review, Drug Development and Industrial Pharmacy. Drug Development and Industrial Pharmacy. https://doi.org/10.3109/03639048709105213.

Yoshioka, S., Miyazaki, T., Aso, Y., 2006. β-relaxation of insulin molecule in lyophilized formulations containing trehalose or dextran as a determinant of chemical reactivity. Pharm. Res. 23, 961–966. https://doi.org/10.1007/s11095-006-9907-3.